Threshold gain behavior of lasing modes in two-dimensional active random media

Chun Wang (王 春), Jinsong Liu (刘劲松), Kejia Wang (王可嘉), Jiantao Lü (吕健滔), Ting Fan (樊 婷), and Hai Liu (刘 海)

State Key Laboratory of Laser Technology, Huazhong University of Science and Technology, Wuhan 430074

Received November 2, 2005

The pumping rate dependence of the peak intensity of the individual lasing mode in two-dimensional (2D) active random media is investigated. The results show that these modes have a typical threshold gain behavior and different threshold pumping rates. There exists a certain correspondence between the mode's threshold pumping rate and its lifetime, and the longer the lifetime is, the lower the threshold is.

OCIS codes: 290.0290, 290.4210, 290.5850, 290.5890, 270.3430.

Coherent feedback random lasers in various strongly[1−3] and weakly[4−6] scattering disordered materials with optical gain show a relatively new research field in the laser action. The random lasing phenomenon was well illustrated with a time dependent theory to perform a lasing numerical simulation in localized modes[7−9]. By use of this theory, the dynamic response and relaxation oscillations in random lasers were analyzed[10], the repulsion and coupling of random lasing modes were studied[11,12], and the morphology, polarized, and temporal dependence of the power spectrum from two-dimensional (2D) random media was investigated theoretically[13−15]. Very recently, random lasing phenomenon was observed in random amplifying layered media[16] and the absorption-induced confinement of lasing modes in diffusive random media was investigated theoretically[17]. The random lasing originating from amplified extended mode was observed and numerically analyzed[18].

Threshold gain behavior is a very important subject for conventional lasers. Although such a subject for random lasers was investigated widely[19−26], the theoretical understanding of this phenomenon remains imperfect. The main conclusions presented are that the lasing threshold pump intensity is inversely proportional to either the square root of the sample area or the square root of the total number of the scatterers, and there is an intermediate particle size at which the threshold pumping energy reaches its minimum. The previous researches on lasing threshold were mainly for whole random lasers, whereas here we pay attention to the individual lasing mode in random lasers. As we know, the lasing modes are identical to the localized modes of the passive media for random lasers[7−9], however, the threshold behavior of the individual localized modes in 2D active random media, so far, has not been investigated yet. In this letter, we study the threshold behavior of localized modes based on the time dependent theory of random lasers[7−9]. Results show that the localized mode has a typical threshold gain behavior, and different modes have different lasing threshold pumping rates. There exists a certain correspondence between the mode's threshold pumping rate and its lifetime, and the longer the lifetime is, the lower the threshold is. However, we have not found there is a certain relationship between the mode's threshold behavior and its localization extent.

We begin with a 2D square disordered medium of size l^2 that is essentially a 2D simplification of real experiments and consists of circular particles with radius r, optical index n_2, and surface-filling fraction Φ. These particles randomly distribute in a background medium with optical index n_1. With these parameters (i.e., r, Φ, n_1, and n_2), large amounts of random media are created. A typical pattern of these random media is shown in Fig. 1.

By combining Maxwell's equations with the rate equations of four-level atomic system, a model was built to describe the random laser phenomena in strongly disordered media in the regime of Anderson localization[7]. For 2D transverse magnetic (TM) field and active medium, Maxwell's equations are[7,8]

$$\mu_0 \partial H_x/\partial t = -\partial E_z/\partial y, \tag{1a}$$

$$\mu_0 \partial H_y/\partial t = \partial E_z/\partial x, \tag{1b}$$

$$\varepsilon_i \varepsilon_0 \partial E_z/\partial t + \partial P/\partial t = \partial H_y/\partial x - \partial H_x/\partial y, \tag{1c}$$

where P is the polarization density, ε_0 and μ_0 are the electric permittivity and the magnetic permeability of vacuum, respectively, and $\varepsilon_i = n_i^2$, $i = 1, 2$. The four-level rate equations are

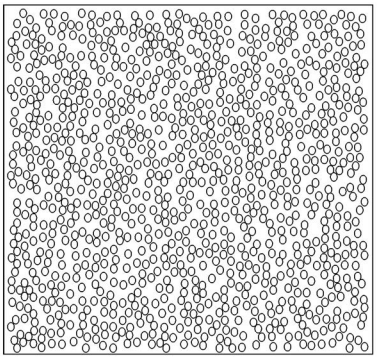

Fig. 1. Random realization of circular particles with $l = 5.5$ μm, $r = 60$ nm, $\Phi = 40\%$, $n_1 = 1$, and $n_2 = 2.3$.

$$dN_1/dt = N_2/\tau_{21} - W_p N_1, \quad (2a)$$

$$dN_2/dt = N_3/\tau_{32} - N_2/\tau_{21} - (E_z/\hbar\omega_l)dP/dt, \quad (2b)$$

$$dN_3/dt = N_4/\tau_{43} - N_3/\tau_{32} + (E_z/\hbar\omega_l)dP/dt, \quad (2c)$$

$$dN_4/dt = -N_4/\tau_{43} + W_p N_1, \quad (2d)$$

where W_p is the pumping rate, N_i is the population density in level i ($i = 1$ to 4), τ_{21}, τ_{32}, and τ_{43} are the lifetime of levels 2, 3, and 4, respectively. The stimulated transition rate is given by the term $(E_z/\hbar\omega_l)dP/dt$, where ω_l is the transition frequency between levels 2 and 3. The polarization density satisfies

$$d^2P/dt^2 + \Delta\omega_l dP/dt + \omega_l^2 P = \kappa \Delta N E_z, \quad (3)$$

where $\Delta N = N_2 - N_3$ is the population density difference between levels 2 and 3, $\kappa = 6\pi\varepsilon_0 c^3/(\omega_l^2 \tau_{32})$, and $\Delta\omega_l = 1/\tau_{32} + 2/T_2$ denotes the linewidth of the atomic transition, in which T_2 is the collision time. The values of parameters that will be used in the following numerical simulations are taken as the same as that listed in Ref. [8]. That is, $T_2 = 2\times10^{-14}$ s, $N_T = \sum_{i=1}^{4} N_i = 3.313\times10^{24}$ m^{-3}, $\tau_{21} = 5\times10^{-12}$ s, $\tau_{32} = 10^{-10}$ s, $\tau_{43} = 10^{-13}$ s, and $\nu_l = \omega_l/2\pi = 6.45\times10^{14}$ Hz.

By setting $P = 0$, the electromagnetic field can be calculated by use of the finite-different time-domain (FDTD) methods to solve the Maxwell's equations with a perfectly matched layer (PML) absorbing condition in order to model an open system[27]. Using a space increment $\Delta x = \Delta y = 10$ nm, the time increment has been chosen to be $\Delta t = \Delta x/(2c) \approx 1.667\times10^{-17}$ s. In order to excite the passive system, a Gaussian electromagnetic pulse of arbitrary amplitude and of duration of about 10^{-16} s is launched. The impulse response is recorded during a time window of length T_w at all nodes in the system and Fourier transformed in order to obtain the intensity spectrum, as shown in Fig. 2. Such a spectrum only exhibits a frequency window of modes at about 645 THz, which corresponds to $\lambda = 464.5$ nm, and this window is only a part of corresponding full spectrum[8,9]. There are many peaks in the spectrum and the number of the peaks is dependent on the recording duration T_w. When T_w is long enough, such as $T_w = 6$ ps, there are a few peaks corresponding to those long-life modes remaining in the spectrum[28,29].

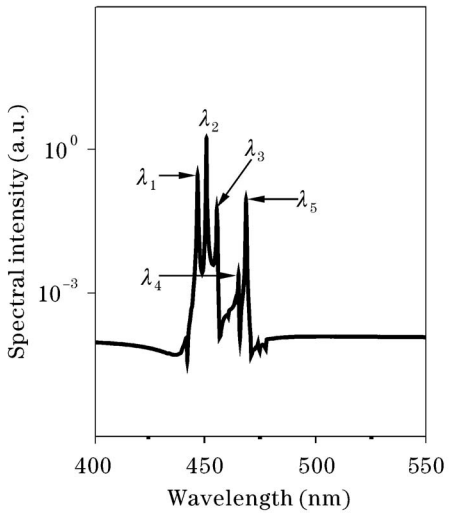

Fig. 2. The spectrum intensity versus the wavelength for the 2D passive random medium shown in Fig. 1 at $T_w = 6$ ps (λ_1 = 447.04 nm, λ_2 = 451.04 nm, λ_3 = 455.74 nm, λ_4 = 465.45 nm, and λ_5 = 468.78 nm).

In order to investigate the mode's threshold properties, we mark five long-life modes in Fig. 2, track their peak intensity (i.e., the intensity at the resonant wavelength) and analyze their threshold gain behavior by supplying a uniform pumping over the whole random system under different pumping rates. Then we obtain the curve of the peak intensity varying with the pumping rate for each mode, as shown in Fig. 3. From it, we can see that the localized modes present a typical threshold gain behavior, and different modes have different lasing threshold pumping rates, in which the mode 5 has the lowest one, the mode 3 has the strongest one.

A question to address here is whether there is a correspondence between the mode's threshold behavior and its localization extent. Considering that the mode's localization extent can be reflected by its spatial distribution, the spatial maps (not shown here) of the five modes are obtained by separately exciting them by a monochromatic source at the resonant frequencies measured in the intensity spectrum. The localization length ξ, which can directly reflect the localization extent, is obtained from these maps by use of a method proposed by Vanneste *et al.*[8,9]. However, as a 2D map, the number of ξ is infinity because it can be measured along any section of map[8,9]. So we have to calculate the values of ξ with 1-degree angular interval and obtain 180 values for each mode. By averaging such 180 values, we obtain the average localization length $\bar{\xi}$ for modes 1 to 5 measured in micron as 0.97, 0.69, 0.79, 0.84, and 0.73, respectively. The relation between $\bar{\xi}$ and the threshold pumping rate W_{pth} is illustrated in Fig. 4. Obviously, there is not a certain correspondence between $\bar{\xi}$ and W_p. This is understandable because the other factors, such as the area, the crowding level or the center location of the map, can also affect the lasing threshold. In other words, the threshold of random lasing modes is determined by many factors, instead of the localization length alone.

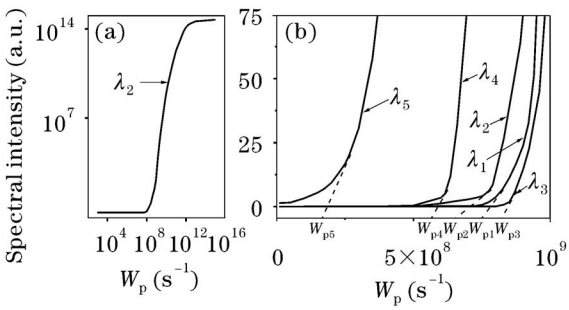

Fig. 3. The pumping rate dependence of the peak intensity of the five modes in the active system. (a) An unbroken view for mode λ_2, (b) part views for the five modes used to compare the threshold pumping rates with each other. The threshold pumping rates of the five modes are $W_{p1} = 7.5\times10^8$ s^{-1}, $W_{p2} = 6.5\times10^8$ s^{-1}, $W_{p3} = 8.2\times10^8$ s^{-1}, $W_{p4} = 5.7\times10^8$ s^{-1}, and $W_{p5} = 1.7\times10^8$ s^{-1}, respectively.

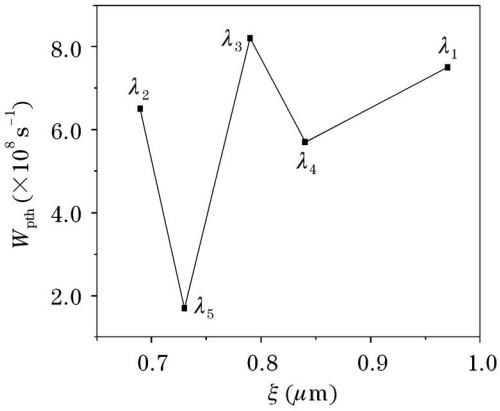

Fig. 4. The correspondence between the mode's threshold pumping rate $W_{\rm pth}$ and its localization length ξ.

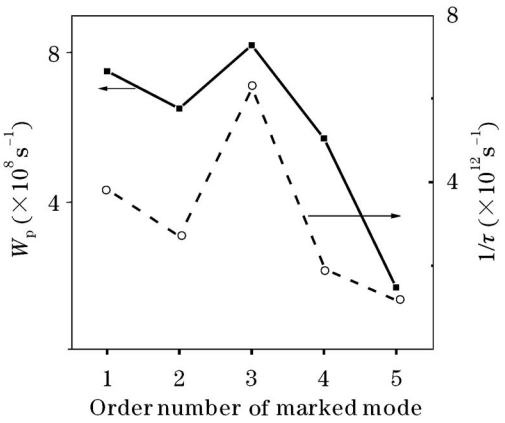

Fig. 6. The relationship between the mode's threshold pumping rate and its lifetime.

In order to find the intrinsic reason that makes the modes be of different threshold pumping rates, we calculate the rate of the energy decay for each marked mode. The five modes are separately excited by a monochromatic source at the resonant frequencies measured in the spectrum shown in Fig. 2 for the passive system. The monochromatic source has a Gaussian envelope with its amplitude to be the same for the five modes. For each mode, the energy is recorded at all nodes and the total energy is obtained by summing the energy at all nodes. Figure 5 shows the evolution of the normalized total energy decay with time, from which we can obtain the mode's lifetime τ for each mode if we define τ to be the time that the total energy decreases from its maximal value $E_{\max}$ to $E_{\max}/\mathrm{e}$. Comparing Fig. 5 with Fig. 3, we can see that the longer the lifetime is, the lower the threshold is. In other words, there is a certain correspondence between the mode's threshold and its lifetime, as shown in Fig. 6. Because the quality factor of a mode is directly proportional to τ, i.e., $Q = 2\pi c\tau/\lambda$, there exists a certain correspondence between the mode's threshold pumping rate and its Q-factor and a localized mode with a larger Q-factor has a lower threshold.

In summary, we have studied numerically the threshold property of the individual localized modes in 2D random media. These localized modes have a typical threshold gain behavior and different modes have different lasing threshold pumping rates. There exists a certain correspondence between the mode's threshold pumping rate and its quality factor, and the larger the Q-factor is, the lower the threshold is.

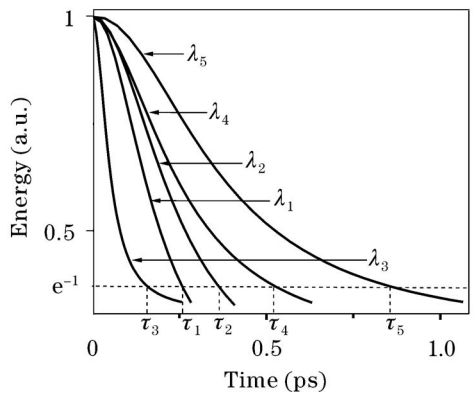

Fig. 5. The normalized total energy decays with time for each marked mode. The five lifetimes are $\tau_1 = 0.26$ ps, $\tau_2 = 0.37$ ps, $\tau_3 = 0.16$ ps, $\tau_4 = 0.52$ ps, and $\tau_5 = 0.86$ ps, respectively.

By defining the lasing threshold pumping rate of a whole random laser as either the minimal threshold among the localized modes or the average one of a set of localized modes, we will have chance to investigate the threshold gain behavior of a whole 2D random laser under different parameters (such as the sample area, the total number of the scatterers, or the particle size), thus comparing our results with experimental ones[6,19–21,25] as well as with that predicted by other theoretical models[6,22–25].

This work was supported by the National Natural Science Foundation of China (No. 60378001), and the Key Program of the Natural Science Foundation of Hubei Province (No. 2001ABA003). J. Liu is the author to whom the correspondence should be addressed, his e-mail address is jsliu4508@vip.sina.com. C. Wang's e-mail address is sunli717@163.com.

References

1. H. Cao, Y. G. Zhao, H. C. Ong, S. T. Ho, J. Y. Dai, J. Y. Wu, and R. P. H. Chang, Appl. Phys. Lett. **73,** 3656 (1998).
2. H. Cao, Y. G. Zhao, S. T. Ho, E. W. Seelig, Q. H. Wang, and R. P. H. Chang, Phys. Rev. Lett. **82,** 2278 (1999).
3. H. Cao, J. Y. Xu, D. Z. Zhang, S.-H. Chang, S. T. Ho, E. W. Seelig, X. Liu, and R. P. H. Chang, Phys. Rev. Lett. **84,** 5584 (2000).
4. R. C. Polson and Z. V. Vardeny, Phys. Rev. B **71,** 045205 (2005).
5. D. Anglos, A. Stassinopoulos, R. N. Das, G. Zacharakis, M. Psyllaki, R. Jakubiak, R. A. Vaia, E. P. Giannelis, and S. H. Anastasiadis, J. Opt. Soc. Am. B **21,** 208 (2004).
6. T. Ling, H. Cao, A. L. Burin, M. A. Ratner, X. Liu, and R. P. H. Chang, Phys. Rev. A **64,** 063808 (2001).
7. X. Jiang and C. M. Soukoulis, Phys. Rev. Lett. **85,** 70 (2000).
8. C. Vanneste and P. Sebbah, Phys. Rev. Lett. **87,** 183903 (2001).
9. P. Sebbah and C. Vanneste, Phys. Rev. B **66,** 144202 (2002).

10. C. M. Soukoulis, X. Jiang, J. Y. Xu, and H. Cao, Phys. Rev. B **65,** 041103 (2002).
11. H. Cao, X. Jiang, Y. Ling, J. Y. Xu, and C. M. Soukoulis, Phys. Rev. B **67,** 161101 (2003).
12. X. Jiang, S. Feng, C. M. Soukoulis, J. Zi, J. D. Joannopoulos, and H. Cao, Phys. Rev. B **69,** 104202 (2004).
13. J. Liu, C. Wang, J. Lu, H. Liu, T. Fan, K. Wang, and H. Wang, Phys. Lett. A **333,** 395 (2004).
14. C. Wang and J. Liu, Phys. Lett. A **353,** 269 (2006).
15. J. Liu, H. Liu, and C. Wang, Acta Phys. Sin. (in Chinese) **54,** 3116 (2005).
16. V. Milner and A. Z. Genack, Phys. Rev. Lett. **94,** 073901 (2005).
17. A. Yamilov, X. Wu, H. Cao, and A. L. Burin, Opt. Lett. **30,** 2430 (2005).
18. S. Mujumdar, M. Ricci, R. Torre, and D. S. Wiersma, Phys. Rev. Lett. **93,** 053903 (2004).
19. G. V. Soest, M. Tomita, and A. Lagendijk, Opt. Lett. **24,** 306 (1999).
20. M. Bahoura, K. J. Morris, and M. A. Noginov, Opt. Commun. **201,** 405 (2002).
21. M. A. Noginov, N. Noginova, S. U. Egarievwe, H. J. Caulfield, C. Cochrane, J. C. Wang, M. R. Kokta, and J. Paitz, Opt. Mater. **10,** 297 (1998).
22. A. L. Burin, M. A. Ratner, H. Cao, and R. P. H. Chang, Phys. Rev. Lett. **87,** 215503 (2001).
23. A. L. Burin, M. A. Ratner, H. Cao, and R. P. H. Chang, Phys. Rev. Lett. **88,** 093904 (2002).
24. M. Patra, Phys. Rev. E **67,** 016603 (2003).
25. M. A. Noginov, G. Zhu, A. A. Frantz, J. Novak, S. N. Williams, and I. Fowlkes, J. Opt. Soc. Am. B **21,** 191 (2004).
26. N. Mikhail, *Solid-State Random Lasers* (Springer, New York, 2005).
27. A. Taflove, *Computational Electrodynamics: The Finite Difference Time Domain Method* (Artech House, Norwood, 1995).
28. S. Yan, Chin. Opt. Lett. **3,** 249 (2005).
29. X. Liu and Y. Wang, Chin. Opt. Lett. **3,** 57 (2005).